4-2010

Magnetoresistance and Magnetocaloric Effect at a Structural Phase Transition from a Paramagnetic Martensitic State to a Paramagnetic Austenitic State in Ni50Mn36.5In13.5 Heusler Alloys

Arjun K. Pathak
Southern Illinois University Carbondale

Igor Dubenko
Southern Illinois University Carbondale

Christopher Pueblo
Southern Illinois University Carbondale

Shane Stadler
Louisiana State University

Naushad Ali
Southern Illinois University Carbondale

Published in *Applied Physics Letters*, Vol. 96 No. 17 (2010) at doi: 10.1063/1.3422483

Magnetoresistance and magnetocaloric effect at a structural phase transition from a paramagnetic martensitic state to a paramagnetic austenitic state in $Ni_{50}Mn_{36.5}In_{13.5}$ Heusler alloys

Arjun K. Pathak,[1,a)] Igor Dubenko,[1] Christopher Pueblo,[1] Shane Stadler,[2] and Naushad Ali[1]
[1]*Department of Physics, Southern Illinois University Carbondale, Illinois 62901, USA*
[2]*Department of Physics and Astronomy, Louisiana State University, Baton Rouge, Louisiana 70803, USA*

(Received 27 February 2010; accepted 11 April 2010; published online 27 April 2010)

It is established, using magnetization measurements, that $Ni_{50}Mn_{36.5}In_{13.5}$ is in a paramagnetic state (PS) above and below the martensitic transition temperature (T_M). Magnetoresistance (MR) and magnetic entropy changes (ΔS_M) in the vicinity of T_M were studied. MR and ΔS_M at T_M were found to be $\approx -8\%$ and $\approx +24$ J Kg^{-1} K^{-1}, respectively, at $\Delta H = 5$ T. Although MR and ΔS_M values were lower than compared to those found in other Heusler systems, the significantly smaller hysteresis observed in $Ni_{50}Mn_{36.5}In_{13.5}$ makes this compound, and other such compounds that undergo a martensitic transition in a PS, promising for the study and applications of magnetocaloric magnetic materials. © *2010 American Institute of Physics*. [doi:10.1063/1.3422483]

Magnetocaloric materials that show large magnetic entropy (ΔS_M) and adiabatic temperature changes [i.e., large magnetocaloric effects (MCE)] with low hysteretic losses are sought for magnetic refrigeration technology. This technology has many advantages over conventional cooling technologies from environmental and energy efficiency perspectives.[1] The MCE results from changes in the magnetic order of materials and, therefore, the most appreciable MCE can be expected in the vicinity of magnetic phase transitions induced by temperature and/or magnetic fields. The value of the MCE depends on the difference in the magnetic state before and after the transition, and on the nature of the transition [being strongest for first-order transitions (FOT)].[2–4]

The giant magnetic entropy changes associated with a change in magnetic moment at the martensitic FOT have been observed in Heusler alloys for the following types of magnetic transitions: (i) paramagnetic-ferromagnetic transitions in Ni–Mn–Ga based Heusler alloys;[5] and (ii) ferromagnetic-antiferromagnetic/paramagnetic transitions in off-stoichiometric Ni–Mn–X (X=In,Sb,Sn) based Heusler alloys.[6–8] However, these systems possess large hysteresis losses and are therefore less effective from an application point of view.

It was previously shown that the temperature of the phase transitions and the magnetic state of the martensitic phases (MP) can be controlled through changing the Mn/In ratio in the $Ni_{50}Mn_{50-x}In_x$ system.[9–11] Therefore, one can assume that the paramagnetic-paramagnetic phase transition at T_M can be observed for some value of x in $Ni_{50}Mn_{50-x}In_x$. The improvement in MCE parameters can be expected in such compounds when the austenitic and MP are both in paramagnetic states.

In this paper, we report the large magnetoresistance and magnetic entropy changes associated with paramagnetic-paramagnetic transition resulting from a structural martensitic transformation in off-stoichiometric $Ni_{50}Mn_{50-x}In_x$ (x=13.5) Heusler Alloys.

Approximately 5 g polycrystalline $Ni_{50}Mn_{36.5}In_{13.5}$ ingot was fabricated by conventional arc melting in an argon atmosphere using high purity (Ni: 99.9%; Mn: 99.99%; and In: 99.9999%) elements. The samples were annealed and the phase purity, crystal structures were determined by the method described in Ref. 9. The magnetic properties were measured by the method described in Ref. 9. The $\Delta S_M(T,H)$ was calculated from isothermal magnetization curves using the Maxwell equation.[9,12] The refrigeration capacity (RC) was calculated by integrating the $\Delta S_M(T,H)$ curves over the full width at half maximum.[9,12]

Room temperature x-ray diffraction measurements revealed that the sample was in mixed modulated martensitic 10 M and austenitic phases (AP) (see Fig. 1 and Ref. 3). The zero-field-cooled (ZFC) heating and cooling magnetization M(T) curves in an external magnetic field (H=0.01 T) are shown in Fig. 2(a). It was observed in the ZFC heating M(T) curve that the magnetization starts to increase at $T \approx 70$ K. From this point, as the temperature increases, the sample

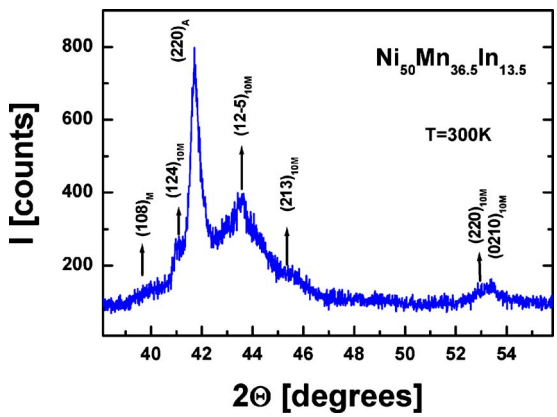

FIG. 1. (Color online) Room temperature XRD patterns of $Ni_{50}Mn_{36.5}In_{13.5}$. The indexes of (hkl) for modulated 10 M and AP are represented by M and A, respectively.

a)Electronic mail: pathak@siu.edu.

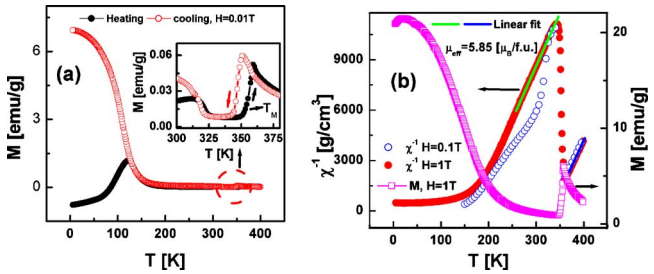

FIG. 2. (Color online) (a) ZFC heating and cooling magnetization [M(T)] at H=0.01 T for $Ni_{50}Mn_{36.5}In_{13.5}$ and (b) ZFC heating M(T) at H=1 T and inverse dc susceptibility at H=0.1 and 1 T of $Ni_{50}Mn_{36.5}In_{13.5}$. Inset of (a) shows the magnified M(T) of the circled region at H=0.01 T.

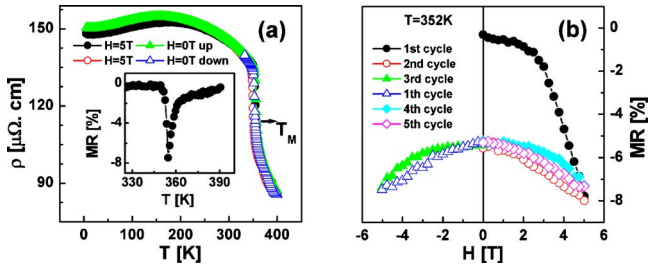

FIG. 3. (Color online) (a) Resistivity as a function of temperature at zero and 5 T external magnetic field for $Ni_{50}Mn_{36.5}In_{13.5}$. The inset shows magnetoresistance as a function of temperature. (b) The magnetoresistance as a function of external magnetic field for consecutive field cycles for $Ni_{50}Mn_{36.5}In_{13.5}$.

undergoes at least two transitions: (i) the Curie transition of the MP (T_{CM}) at $T \approx 133$ K and (ii) the martensitic transition at temperature $T_M \approx 358$ K [see inset of Fig. 2(a)]. Similarly, while decreasing the temperature [ZFC cooling M(T)], the samples passes the martensitic transition temperature $T_M \approx 347$ K, detected from a jumplike decrease in magnetization. The clear presence of a hysteretic effect of 11 K in the transition temperatures of the ZFC heating and cooling M(T) curves [see inset of Fig. 2(a)] at T_M is evidence of a FOT. Also, as shown in Fig. 2(a), the ZFC heating and cooling M(T) curves split at $T \approx 125$ K. It is interesting to note that a similar splitting in magnetization curves has also been observed in other systems due to the presence of inhomogeneous magnetic states at low temperature resulting in the exchange bias phenomena.[13–15]

In order to clarify the magnetic behavior, ZFC magnetization measurements [M(T)] were carried out for applied magnetic fields of H=0.1 and 1 T. Inverse susceptibility $\chi^{-1}=H/M$ curves are shown in Fig. 2(b). It can be seen that the applied H=1 T does not provide a visible shift in the martensitic transition temperature ($T \approx 358$ K). The magnitude of $\chi^{-1}(T)$ at H=0.01 T is approximately the same as that for H=1 T. In addition, the slopes of $\chi^{-1}(T)$ are equal [see linear fit in Fig. 2(b)] in both regions $T > T_M$ and $T < T_M$, respectively. A small deviation from linearity in $\chi^{-1}(T)$ is observed at H=0.01 T below 320 K. This low field behavior of $\chi^{-1}(T)$ below T_M most likely results from a small amount of ferromagnetic impurity, considering that $\chi^{-1}(T)$ at 1 T is a purely linear function in the temperature interval $200\ K < T < T_M$ [see Fig. 2(b)]. The observed $\chi^{-1}(T)$ in $T > T_M$ and $T < T_M$ regions suggests that the sample is in a PS above and below T_M (in a certain temperature interval). Thus, for $Ni_{50}Mn_{36.5}In_{13.5}$, T_M exceeds the Curie temperature of the AP, T_C, and the compound undergoes a FOT from the paramagnetic martensitic state (PMS) to a paramagnetic austenitic state (PAS) at $T_M=358$ K (while heating). The effective paramagnetic moments (μ_{eff}) and paramagnetic Curie temperatures (θ_P) were found to be 5.85 μ_B/f.u., 172 K (martensitic), and 334 K (austenitic), respectively.

The electrical resistivity (ρ) at zero and 5 T external magnetic field are shown in Fig. 3(a). In both cases, ρ increases almost linearly with increasing temperature, and sharply decreases in the vicinity of T_M. As observed in the magnetization measurements (Fig. 2), a small hysteresis was also observed in ρ measurements, which is typical for a FOT. A small shift of T_M to lower temperature (of about 5 K) can be seen from the comparison of $\rho(T)$ at H=0 and 5 T [see Fig. 3(a)].

The MR was determined by $MR(T)=\{[\rho(H,T)-\rho(0,T)]/\rho(0,T)\}\times 100\%$. The maximum MR was found to be $\approx -8\%$ for H=5 T. This obtained value of MR(T) was confirmed by MR measurements as a function of external magnetic field, the MR(H), at T=352 K. As shown in Fig. 3(b), with the increasing external magnetic field, the MR(H) increases and reaches a maximum value of $\approx -8\%$ in the paramagnetic phase. However, upon removing the field, original MR could not be recovered. The application of a magnetic field results in the decrease in MR at H=0 after the first cycle. The resistivity of the AP is less than that of the MP at H=0 [see Fig. 3(a)]. Thus, it is reasonable to assume that the application of a magnetic field results in an increase in the amount of AP in the vicinity of T_M. These effects are similar to that observed in other systems, where the phenomenon was explained as a field arrested state across the martensitic transition.[16,17]

Figure 4 shows the magnetization curves at discrete temperatures in increasing and decreasing fields up to 5 T. As seen in from Fig. 4, the magnetization curves are linear functions of magnetic field for both regions, $T > T_M$ and $T < T_M$, and show metamagnetic types of behavior at $T \sim T_M$ [see M(H) at 347–349 K in Fig. 4]. Thus, the small difference in magnetization of the MP and AP in paramagnetic states is sufficient to make the AP preferable at high external magnetic fields.

The hysteresis loss (HL) was estimated by calculating the area enclosed by the magnetizing and demagnetizing M(H) curves (see in inset of Fig. 4). Although Maxwell's

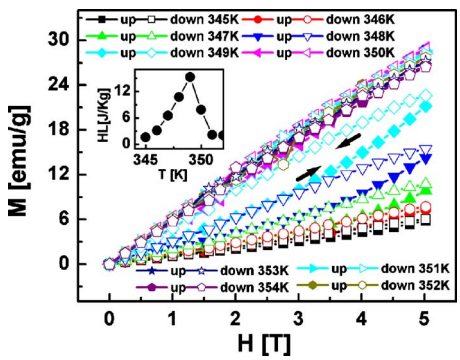

FIG. 4. (Color online) (a) Isothermal magnetization curves M(H) for $Ni_{50}Mn_{36.5}In_{13.5}$ in the vicinity of the FOT. Arrows show the hysteresis loops in the vicinity of the FOT. The inset shows the hysteretic loss HL in the vicinity of the FOT.

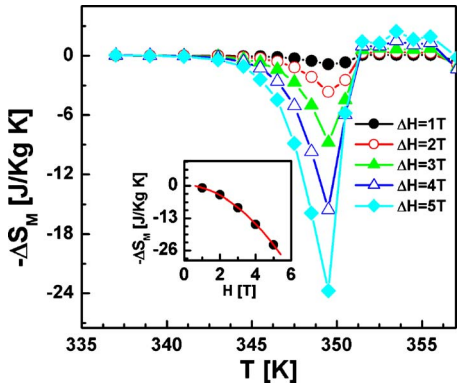

FIG. 5. (Color online) (a) Magnetic entropy change (ΔS_M) in $Ni_{50}Mn_{36.5}In_{13.5}$ with temperature in the vicinity of the FOT. The inset shows the ΔS_M as a function of applied magnetic field.

equation[9,12] is valid only for second order magnetic transitions to calculate ΔS_M, as suggested by Gschneidner *et al.*[12] and Casanova *et al.*,[18] it is conventionally employed to calculate ΔS_M in the vicinity of FOT's. As shown in Figs. 2 and 4, the M(T,H) does not possess any problematic discontinuities. Therefore, we have used the Maxwell equation to estimate ΔS_M in the vicinity of the FOT. Figure 5 shows the positive (i.e., inverse) entropy change in the vicinity of the FOT. The maximum ΔS_M was found to be $\approx$+24 J Kg^{-1} K^{-1} at T=350 K for ΔH=5 T. This value of ΔS_M is comparable to other magnetocaloric materials $Ni_{50}Mn_{35}In_{15}$ (+25 J Kg^{-1} K^{-1} at T=301 K, H=5 T),[19] $Ni_{46}Mn_{41}In_{13}$ (+13.5 J Kg^{-1} K^{-1} at T=190 K, H=5 T) (Ref. 20) which undergo martensitic transformation from low magnetic state to ferromagnetic AP. The ΔS_M was found to increase almost linearly with external magnetic field (see inset of Fig. 5). As can be seen from Fig. 5, the large value of ΔS_M was found in the vicinity of the PMS and PAS. Other important parameters to evaluate the potential of the MCE of a given material are the RC and the hysteretic loss. The maximum RC was found to be 39 J/Kg. As shown in the inset of Fig. 4, the HL was found to be a maximum at the same temperature (349 K) as that of the maximum of the ΔS_M curve (see Fig. 5). The average HL $\approx$8 J/Kg was calculated over the same temperature range as that of the full width half maximum of the ΔS_M. The net RC was calculated by subtracting the average HL and was found to be RC (net) 31 J/Kg.

In conclusion, although the obtained values of MCE and MR are lower than recently reported values in other Heusler systems, very small HL and improved reversibility of MCE parameters observed in $Ni_{50}Mn_{50-x}In_x$ (x=13.5) makes it a promising material to study for magnetic refrigeration systems. However, although giant ΔS_M and large RC were previously reported in the vicinity of paramagnetic–ferromagnetic transitions or ferromagnetic–antiferromagnetic/paramagnetic transitions, large hysteretic effects (temperature and field dependence) were also associated with such materials. On the other hand, the second order transition possesses a small value of ΔS_M. Therefore, magnetic materials that exhibit large ΔS_M with low hysteretic losses associated with a FOT from PMS-PAS are desirable for possible application in magnetic refrigeration technology.

This research was supported by a Research Opportunity Award from Research Corporation (RA-0357), and by the Office of Basic Energy Sciences, Material Sciences Division of the U.S. Department of Energy (Contract No. DE-FG02-06ER46291).

[1]K. A. Gschneidner, Jr., and V. K. Pecharsky, Int. J. Refrig. **31**, 945 (2008).
[2]V. K. Pecharsky and K. A. Gschneidner, Jr., Phys. Rev. Lett. **78**, 4494 (1997).
[3]T. Krenke, E. Duman, M. Acet, E. F. Wassermann, X. Moya, L. Mañosa, and A. Planes, Phys. Rev. B **75**, 104414 (2007).
[4]H. Wada and Y. Tanabe, Appl. Phys. Lett. **79**, 3302 (2001).
[5]S. Stadler, M. Khan, J. Mitchell, N. Ali, A. M. Gomes, I. Dubenko, A. Y. Takeuchi, and A. P. Guimarães, Appl. Phys. Lett. **88**, 192511 (2006).
[6]X. Moya, L. Mañosa, A. Planes, S. Aksoy, M. Acet, E. F. Wassermann, and T. Krenke, Phys. Rev. B **75**, 184412 (2007).
[7]I. Dubenko, M. Khan, A. K. Pathak, B. R. Gautam, S. Stadler, and N. Ali, J. Magn. Magn. Mater. **321**, 754 (2009).
[8]A. K. Pathak, I. Dubenko, S. Stadler, and N. Ali, J. Phys. D **41**, 202004 (2008).
[9]A. K. Pathak, M. Khan, I. Dubenko, S. Stadler, and N. Ali, Appl. Phys. Lett. **90**, 262504 (2007).
[10]A. K. Pathak, M. Khan, B. R. Gautam, S. Stadler, I. Dubenko, and N. Ali, J. Appl. Phys. **103**, 07F315 (2008).
[11]A. K. Pathak, I. Dubenko, S. Stadler, and N. Ali, J. Appl. Phys. **105**, 07B103 (2009).
[12]K. A. Gschneidner, Jr., V. K. Pecharsky, and A. O. Tsokol, Rep. Prog. Phys. **68**, 1479 (2005).
[13]A. K. Pathak, M. Khan, B. R. Gautam, S. Stadler, I. Dubenko, and N. Ali, J. Magn. Magn. Mater. **321**, 963 (2009).
[14]M. Khan, I. Dubenko, S. Stadler, and N. Ali, Appl. Phys. Lett. **91**, 072510 (2007).
[15]A. K. Pathak, I. Dubenko, S. Stadler, and N. Ali, IEEE Trans. Magn. **45**, 3855 (2009).
[16]S. Chatterjee, S. Giri, S. Majumdar, and S. K. De, Phys. Rev. B **77**, 012404 (2008).
[17]A. K. Pathak, I. Dubenko, S. Stadler, and N. Ali, J. Phys. D **42**, 045004 (2009).
[18]F. Casanova, X. Batlle, A. Labarta, J. Marcos, L. Mañosa, and A. Planes, Phys. Rev. B **66**, 100401 (2002).
[19]P. A. Bhobe, K. R. Priolkar, and A. K. Nigam, Appl. Phys. Lett. **91**, 242503 (2007).
[20]K. Oikawa, W. Ito, Y. Imano, Y. Sutou, R. Kainuma, K. Ishida, S. Okamoto, O. Kitakami, and T. Kanomata, Appl. Phys. Lett. **88**, 122507 (2006).